PHYSICAL REVIEW B VOLUME 57, NUMBER 16 15 APRIL 1998-II

Al/ZnSe(100) Schottky-barrier height versus initial ZnSe surface reconstruction

M. Lazzarino, G. Scarel, S. Rubini, G. Bratina, L. Sorba,* and A. Franciosi
Laboratorio Nazionale TASC-INFM, Padriciano 99, I-34012 Trieste, Italy
and Department of Chemical Engineering and Materials Science, University of Minnesota, Minneapolis, Minnesota 55455

C. Berthod, N. Binggeli, and A. Baldereschi
Institut de Physique Appliquée, Ecole Polytechnique Fédérale de Lausanne, CH-1015 Lausanne, Switzerland
(Received 22 September 1997)

Al/ZnSe(100) Schottky barriers fabricated on $c(2\times2)$, 2×1, and 1×1 reconstructed surfaces were studied by means of photoemission spectroscopy and first-principles calculations. Relatively similar values of the Schottky barriers were found for interfaces fabricated on Zn-stabilized $c(2\times2)$ and Se-dimerized 2×1 surfaces, while substantially lower values of the p-type barriers were predicted theoretically and observed experimentally for junctions grown on the Se-rich 1×1 surface. [S0163-1829(98)51716-X]

The possibility of tuning the Schottky-barrier height has been attracting attention since the inception of the study of metal/semiconductor junctions.[1] Recently, renewed interest has been stimulated by the contact problems that plague wide-band-gap semiconductors such as ZnSe and GaN.[2–7]

We report experimental and theoretical studies of the Schottky barrier at Al/ZnSe(100) interfaces showing that the barrier height is strongly dependent on the initial composition of the semiconductor surface. The observed experimental trend is that while the $c(2\times2)$ and 2×1 surface terminations correspond to similar barrier heights, a 0.25 ± 0.05 decrease in the p-type barrier is found when the junction is fabricated on the Se-rich 1×1 surface termination. The theoretical trend in the barrier is compellingly similar, i.e., junctions corresponding to the $c(2\times2)$ and 2×1 terminations are predicted to have relatively similar barrier heights (within 0.05 eV), while those obtained for the Se-rich 1×1 surface are expected to have a lower p-type barrier, and specifically lower by 0.45 ± 0.20 eV for the measured excess Se coverage of 0.41 ± 0.18 ML of the 1×1 relative to the 2×1 reconstruction. Our first-principles calculations for model interface configurations explain our experimental results in terms of a variable Se-induced local interface dipole.

ZnSe epilayers (500 nm thick) were grown by molecular-beam epitaxy (MBE) on GaAs(100).[8] All epilayers were Cl doped ($n\sim1-3\times10^{18}$ cm^{-3}). A thick Se cap layer was used to protect the samples during transfer in air to the photoelectron spectrometer. The Se cap layer was thermally desorbed *in situ*, and different surface reconstructions—as determined by reflection high-energy electron diffraction (RHEED)—were obtained by varying the annealing conditions. Al overlayers 2–3 nm thick were evaporated *in situ* on ZnSe substrates kept at room temperature, with thickness determined using a quartz thickness monitor. Surfaces and interfaces were examined after quenching to room temperature by monochromatic x-ray photoemission spectroscopy (XPS) using Al $K\alpha$ radiation (1486.6 eV), an overall energy resolution (electron plus photons) of ~0.8 eV, and an effective photoelectron escape depth of ~1.5 nm, or by soft-x-ray synchrotron radiation photoemission spectroscopy (SRPES) at the Synchrotron Radiation Center of the University of Wisconsin–Madison, with an energy resolution of 0.2 eV.

In Fig. 1 we show SRPES results for the Se $3d$ and Zn $3d$ core-level emission at a photon energy of 120 eV from surfaces exhibiting the three types of RHEED patterns reproducibly obtained in sequence upon annealing. After annealing at ~260 °C, the Se-rich 1×1 surface gives rise to a relatively broad Se $3d$ line shape which reflects a high binding-energy contribution associated with Se-Se coordination at the surface,[9] and a Zn $3d$/Se $3d$ integrated intensity ratio $R=0.81\pm0.03$. Following annealing at ~330 °C, the Se-stabilized 2×1 reconstruction gives rise to a sharper Se $3d$ line shape, and a Zn $3d$/Se $3d$ integrated intensity ratio $R=0.95\pm0.03$. This reconstruction is also observed during ZnSe MBE in Se-rich growth conditions, and is believed to correspond to a surface terminated by a fully dimerized monolayer of Se.[9] For higher annealing temperatures ($\geqslant430$ °C), the well-known $c(2\times2)$ reconstruction[9–11] is seen to correspond to a single Se $3d$ doublet, a clearly defined high binding-energy shoulder in the Zn $3d$ line shape, and $R=1.21\pm0.03$. This reconstruction is also observed dur-

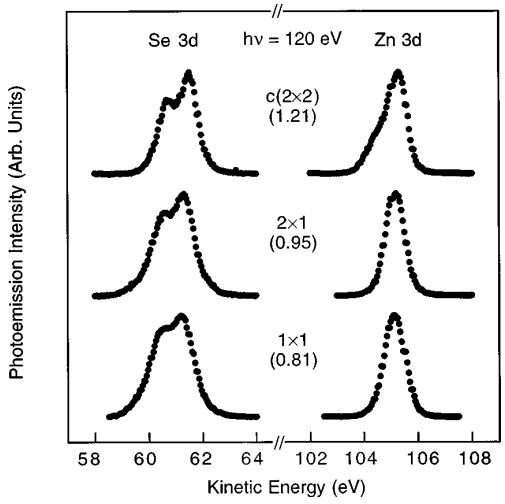

FIG. 1. Synchrotron radiation photoemission (SRPES) results for the Se $3d$ and Zn $3d$ core-level emission from the Se-rich 1×1 (bottom-most spectra), Se-dimerized 2×1 (midsection), and Zn-stabilized $c(2\times2)$ (topmost spectra) reconstructions of the ZnSe(100) surface. The corresponding values of the Zn $3d$/Se $3d$ integrated intensity ratio R are 0.81, 0.95, and 1.21, respectively.

ing ZnSe MBE in Zn-rich growth conditions, and is believed to correspond to a surface terminated by half a monolayer of Zn atoms on a complete ML of Se, i.e., to an ordered array of Zn vacancies within the outermost layer of Zn atoms.[9–11] The shoulder on the low kinetic-energy side of the main bulk-related Zn $3d$ feature, in particular, is believed to be associated with such Zn surface atoms.[9]

Recent total-energy calculations have shown the $c(2\times2)$ and 2×1 reconstructions to be the lowest energy configurations among those examined for Zn-rich and Se-rich surfaces, respectively.[12] In fact, the Se-rich 1×1 reconstruction is not observed during ZnSe MBE, and has only been reported during desorption of a Se cap layer. Kahn and coworkers reported a Se-rich 1×1 reconstruction for an annealing temperature of $\sim$200 °C, and tentatively associated this reconstruction with the presence of 2–3 ML of excess Se on the surface.[9] Lopinsky *et al.* studied the same surface and reported strong similarities between the corresponding electronic states and those observed upon deposition of a single amorphous monolayer of Se onto an unreconstructed, Se-terminated ZnSe surface.[13]

The R values in Fig. 1 were used to model the surface composition under three main simplifying assumptions: (i) a single photoelectron escape depth λ—independent of the surface termination—exists for the bulk and surface regions; (ii) the photoemission intensity can be expressed as the sum of the emission intensities from discrete (100) atomic planes; (iii) the emission from a given plane at a depth d from the surface is attenuated by $e^{-d/\lambda}$. The measured R values are then found to be consistent with an excess Se coverage x of about half a monolayer for the 1×1 surface used in this study as compared to the 2×1 surface[14]

Prior to metal deposition, the positions of the Zn $3d$ and Se $3d$ centroids relative to the valence-band maximum E_V were determined using a least-squares fit and a linear extrapolation of the leading edge of the valence band. Upon deposition of 2–3 nm of Al, new measurements of the core-level positions and the known position of the spectrometer Fermi level E_F were used to infer the p-type Schottky barrier $\Phi_p \sim E_F - E_V$ and the n-type barrier $\Phi_n \sim E_C - E_F$, with $E_C - E_V = 2.70$ eV at room temperature. The procedure is illustrated in Fig. 2. Prior to metal deposition, the centroid of the Zn $3d$ core doublet was found 9.16 ± 0.04 eV below E_V for all surfaces. Upon metal deposition, the Al $2p$ core-level emission appears at the position expected for elemental metallic Al for all interfaces examined. The position of the Zn $3d$ centroid varies instead for the three interfaces, and can be used to infer the position of E_V relative to E_F.

From the results in Fig. 2 we determined $\Phi_n = 0.55 \pm 0.06$ eV ($\Phi_p = 2.15 \pm 0.06$), $\Phi_n = 0.59 \pm 0.06$ ($\Phi_p = 2.11 \pm 0.06$), and $\Phi_n = 0.79 \pm 0.06$ eV ($\Phi_p = 1.91 \pm 0.06$) for interfaces fabricated on $c(2\times2)$, 2×1, and 1×1 reconstructions, respectively. The quoted experimental uncertainty applies to each individual value of the barrier, but the uncertainty on the barrier height *variation* in the series, that depends only on the determination of core-level *shifts*, is comparatively smaller (typically 0.03 eV). Interface reactions do not affect the Schottky-barrier determination in Fig. 2. This is demonstrated by the SRPES results for a junction fabricated on a 1×1 surface in the bottom-most section of Fig. 2. Prior to metal deposition, the position of the Zn $3d$ centroid was found 9.13 ± 0.03 eV below E_V. After metal deposition, the Zn $3d$ line shape shows two contributions. A low binding-energy doublet develops during the early stages of interface formation, and reflects Zn atoms displaced from the semiconductor and segregated in the metallic overlayer. This reacted component is visible as a shoulder in the XPS results, and is emphasized in SRPES due to the higher surface sensitivity. The high binding-energy doublet derives from the ZnSe substrate, and can be used to obtain $\Phi_n = 0.78 \pm 0.04$ eV, in good agreement with the XPS result.

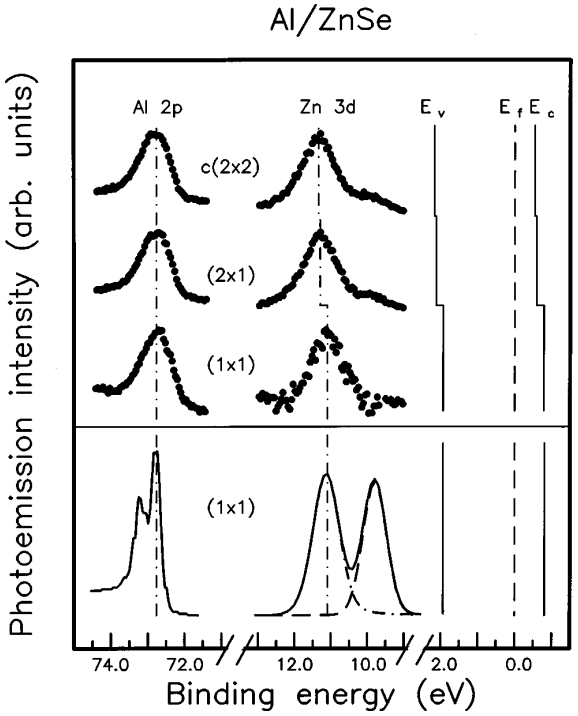

FIG. 2. X-ray photoemission spectroscopy results for the Al $2p$ (left) and Zn $3d$ (center) core-level emission, together with the corresponding position of the Fermi level E_F in the gap for Al/ZnSe(100) junctions fabricated by depositing 3-nm-thick Al overlayers on $c(2\times2)$, 2×1, and 1×1 surface reconstructions (three topmost sections, top to bottom, respectively). For comparison we also show (bottom-most spectra) SRPES results for a junction fabricated on the Se-rich 1×1 reconstruction. The low binding-energy $3d$ doublet (dashed line) reflects Zn atoms within the metallic overlayer. The high binding-energy doublet (dot-dashed line) derives from the semiconductor substrate. The position of the bulk Zn $3d$ emission is used to derive the position of the valence-band maximum E_V and the conduction-band minimum E_C relative to the Fermi level E_F at the interface (right-most section).

Previous determinations of the n-type Schottky barrier for Al/ZnSe junctions focused on the $c(2\times2)$ reconstruction and yielded values of 0.55 ± 0.10 eV (Ref. 15) and 0.58 ± 0.10 eV (Ref. 10), consistent with those reported here for the same reconstruction. The 0.24 eV increase in Φ_n (decrease in Φ_p) for interfaces fabricated on the Se-rich 1×1 reconstruction in Fig. 2 is among the highest barrier changes versus semiconductor reconstruction which have been reported to date.[1] To investigate the microscopic mechanisms that may account for such a large change in the Schottky barrier, we performed first-principles calculations of the band alignment for a series of model interface configurations.

As in recent studies of Al/GaAs(100) junctions,[6] the calculations were performed within the local-density approximation to density-functional theory (DFT), using the pseudopotential plane-wave method.[16] To model the isolated Al/

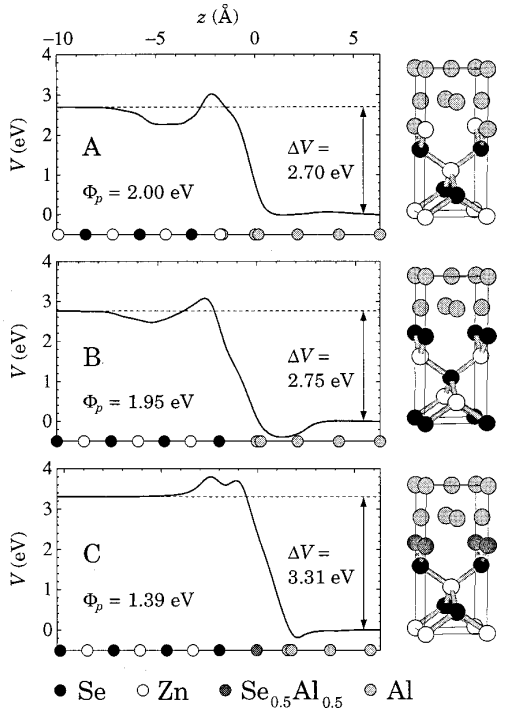

FIG. 3. Right: Starting interface configurations employed in the supercell calculations. Configuration *A* involves Al atoms positioned at the Zn vacancy sites of the $c(2\times2)$ surface, below the Al fcc lattice rotated 45° about the [100] axis relative to ZnSe to satisfy the epitaxial relation. Configuration *B* involves a ZnSe surface terminated by a full Se monolayer below the fcc metal. Configuration *C* involves a ZnSe surface terminated by a 50% Se–50% Al atomic layer on top of a full Se monolayer. Left: Macroscopic average of the electrostatic potential energy *V* and potential energy lineup ΔV across the relaxed junctions. Relaxation is graphically illustrated at the bottom for each atomic plane. Double atomic symbols denote inequivalent relaxation at different sites. Since an increase in ΔV corresponds to an identical decrease in E_F-E_V, the calculations predict a 0.05 eV decrease in Φ_p in going from the relaxed configuration *A* to the relaxed configuration *B*, and a further decrease by 0.56 eV in going from the relaxed configuration *B* to the relaxed configuration *C*. The calculated values of Φ_p are also shown.

ZnSe(001) interfaces, we used supercells consisting of 13 layers of ZnSe and 7 layers of Al. In view of the good lattice matching between ZnSe and GaAs, many of the structural considerations put forth in Refs. 6 also apply to the present case. In particular, the Al [100] direction was made parallel to the ZnSe [100] growth axis, and the Al fcc lattice was rotated 45° about the [100] axis relative to ZnSe cubic lattice in order to satisfy epitaxial relations. The Al overlayer was tetragonally elongated (4%) following macroscopic elasticity theory, and the local atomic structure at the interface was fully relaxed.

The starting interface configurations[17] prior to atomic relaxation are schematically illustrated on the right-hand side of Fig. 3. We selected simple configurations corresponding to ideal continuations of the semiconductor bulk while taking into account the initial composition of the starting surface. For Al/ZnSe fabricated on the $c(2\times2)$ surface we positioned Al atoms at the Zn vacancy sites of the outermost semiconductor layer (configuration *A* in Fig. 3). For Al/ZnSe fabricated on the 2×1 surface we terminated the semiconductor with a full layer of Se atoms at the ideal bulk positions (configuration *B*). For Al/ZnSe fabricated on the 1×1 surface, we used a virtual crystal approach to terminate the semiconductor with a 50% Se-50% Al atomic layer (configuration *C*).

For convenience the Schottky barrier was decomposed as $\Phi_p=\Delta E_p+\Delta V$. The band-structure term ΔE_p is the difference between the Fermi energy of the metal and the valence-band edge of the semiconductor, E_V, in the bulk, each measured relative to the average electrostatic potential of the corresponding crystal.[6] This term does not depend on the interface, and was determined from standard bulk band-structure calculations for ZnSe and Al. The second term ΔV is the electrostatic potential-energy lineup across the interface, and contains all interface-specific features. This is the only term in Φ_p which may change in the presence of interfacial perturbations.

The potential energy lineup ΔV was derived via Poisson's equation from the self-consistent supercell charge density using the macroscopic average technique.[6] The supercell calculations were performed with a plane-wave kinetic-energy cutoff of 20 Ry. The other computational details are as in Ref. 6. In Fig. 3 we show the macroscopic average of the potential energy *V* and the potential lineup across the relaxed junctions. Since an increase in ΔV corresponds to an identical increase in E_C-E_F (decrease in E_F-E_V), the calculations predict a 0.05 eV increase in Φ_n (decrease in Φ_p) in going from the relaxed configuration *A* to the relaxed configuration *B*, and a further increase of Φ_n (decrease in Φ_p) by 0.56 eV in going from the relaxed configuration *B* to the relaxed configuration *C*. The direction and order of magnitude of the predicted shifts are consistent with those observed experimentally (see Fig. 2), suggesting that although the model configurations employed may not describe the detail of the actual atomic reconstructions,[18] they do capture the basic electrostatic trend as a function of interface composition.

We emphasize that atomic relaxation at the Al/ZnSe(100) interfaces is substantial, and has an important effect (of the order of 0.5–1 eV) on the Schottky-barrier height, especially for the Se-rich configuration *C*. In this case, from the initial configuration *C* we found that the Se–$Al_{0.5}Se_{0.5}$ interplanar spacing at the interface increased by 40% after convergence, and became comparable to the $Al_{0.5}Zn_{0.5}$–Al and Se–Al interplanar distances of configurations *A* and *B*, respectively. This large relaxation in configuration *C* reflects the increased metallic character of the bonds between the Se and the $Al_{0.5}Se_{0.5}$ atomic layer.

To calculate Φ_p, the LDA band-structure term E_V and therefore ΔE_p should be corrected to take into account many-body and relativistic effects. As a ground-state property, ΔV is instead accurately determined within DFT. The spin-orbit correction on ΔE_p was derived from experiment, and amounts to -0.15 eV. The many-body corrections to the band structure of ZnSe have been evaluated in Ref. 19. As the LDA band-gap values in our calculations and in Ref. 19 are different, due to the different pseudopotentials employed, we used the valence band-edge correction of Ref. 19 and scaled it by the ratio of the difference between the *GW* band gap[19] and the LDA band gaps in the two calculations. The resulting estimate for the many-body correction on ΔE_p was $+0.50$ eV. Using these two corrections, we obtain $\Phi_p=2.00$, 1.95, and 1.39 eV for the relaxed configurations *A*, *B*, and *C*, respectively. We emphasize that while the *variation* of the calculated Schottky barrier with interface composition is independent on the magnitude of the self-energy

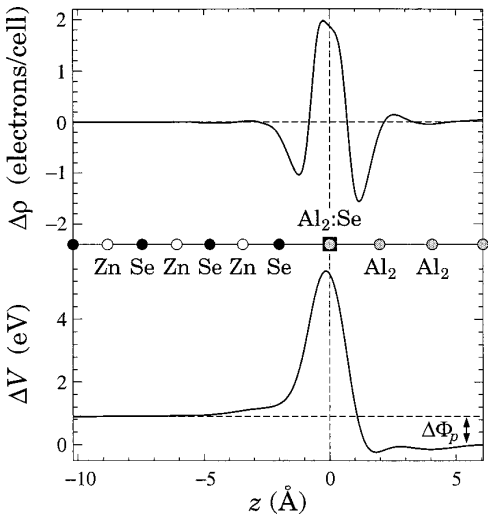

FIG. 4. Difference in the charge distribution (top) and average potential energy (bottom) calculated between an interface terminated with two full Se monolayers, and a single Se monolayer. The latter corresponds to the relaxed configuration *B*, while the former corresponds to the limiting case of a type-*C* configuration for $x>1$.

correction, the absolute value of the barrier depends on the magnitude of such a correction, which was not calculated in our work, but simply rescaled from that of Ref. 19. There is therefore a substantial uncertainty (± 0.2 eV) in the absolute values of the theoretical barrier.

The mechanism responsible for the large reduction in Φ_p for interfaces fabricated on the 1×1 surface is illustrated in Fig. 4, where we plot the difference in the electronic charge distribution and in the electrostatic potential calculated between an interface terminated with two full Se monolayers and a single Se monolayer. The latter corresponds to the relaxed configuration *B*, while the former corresponds to the limiting case of a type-*C* configuration for $x>1$. Charge transfer from both the metal and the Se-terminated semiconductor to the excess Se atoms at the interface is clearly visible, and the asymmetry in the charge transfer gives rise to a well-defined dipole-field across the interface. The dipole-induced change in the electrostatic potential lineup is roughly proportional to the Se excess coverage x on the Se-terminated semiconductor surface for $0<x<1$. A 0.95 eV decrease in Φ_p is obtained for $x=1$ (see Fig. 4), and a 0.56 eV decrease is calculated for $x=0.5$ (Fig. 3). Therefore a 0.45 ± 0.20 eV decrease in the barrier is expected for $x=0.41\pm0.18$ (Ref. 14).

Recently, Chen *et al.* reported a 0.25-eV reduction in the *p*-type barrier for Au/ZnSe(100) junctions by introducing a 2–3 ML Se interlayer between the metal and the semiconductor, and proposed an electronegativity-based interpretation of the barrier reduction.[15] The similar 0.25-eV barrier reduction in the presence of vastly different electronegativity variations ΔX ($\Delta X=0.94$ for Al-Se versus 0.01 for Au-Se in Pauling's scale), and the expected saturation of the dipole in Fig. 4 for $x>1$, call into question the general applicability of a simple electronegativity-based approach. Our results suggest that lattice relaxation plays an important role in determining the Schottky barrier in these systems and should be taken into account to improve upon electronegativity-based estimates of the interface dipole.

In summary, experiment points to an important effect of the initial ZnSe surface composition on the Al/ZnSe(100) Schottky barrier. In particular, the presence of an excess Se coverage x at the 0.5 ML level on top of a fully Se-terminated ZnSe surface gives rise to a local interface dipole that lowers substantially the *p*-type barrier. Theory shows that the dominant related charge transfer occurs from the first Al monolayer to the excess Se atoms, and that the large relaxation of the Se-Se interatomic distance has a major role in determining the actual value of the dipole moment at the interface.

The work in Trieste was supported in part by INFM under the TUSBAR Advanced Research Project. The work in Minneapolis was supported in part by the National Science Foundation under Grant No. DMR-9116436. The work in Lausanne was supported by the Swiss National Science Foundation under Grant No. 20-47065.96. Useful discussions with A. Kahn are gratefully acknowledged.

*Also at Istituto ICMAT del CNR, Montelibretti, Roma, Italy.

[1] See, for example, L. J. Brillson, in *Handbook on Semiconductors*, edited by P. T. Landsberg (Elsevier, Amsterdam, 1992), Vol. 1, p. 281, and R. T. Tung, in *Contacts to Semiconductors*, edited by L. J. Brillson (Noyes Publications, Park Ridge, 1993), p. 176, and references therein.

[2] See, for example, *II-VI Blue/Green Laser Diodes*, edited by Robert L. Gunshor and Arto V. Nurmikko [Proc. SPIE, **2346**, 1 (1991)].

[3] S. N. Mohammed and H. Morkoç, Prog. Quantum Electron. **20**, 361 (1996).

[4] A. Franciosi and C. G. Van de Walle, Surf. Sci. Rep. **25**, 1 (1996).

[5] M. Cantile *et al.*, Appl. Phys. Lett. **64**, 988 (1994); L. Sorba, S. Yildirim, M. Lazzarino, A. Franciosi, D. Chiola, and F. Beltram, *ibid.* **69**, 1927 (1996).

[6] C. Berthod *et al.*, Europhys. Lett. **36**, 76 (1996); C. Berthod, J. Bardi, N. Binggeli, and A. Baldereschi, J. Vac. Sci. Technol. B **14**, 3000 (1996).

[7] S. M. Sze, *Physics of Semiconductor Devices* (Wiley, New York, 1981), p. 304

[8] M. Lazzarino *et al.*, Appl. Phys. Lett. **68**, 370 (1996), and references therein.

[9] A detailed analysis of the evolution of the Se 3*d* and Zn 3*d* line shape as a function of Se desorption has already been presented by W. Chen, A. Kahn, P. Soukiassan, P. S. Mangat, J. Gaines, C. Ponzoni, and D. Olego, Phys. Rev. B **49**, 10 790 (1994). The purpose of Fig. 1 is to calibrate the composition of the actual surfaces employed in the present study.

[10] M. Vos *et al.*, Phys. Rev. B **39**, 10 744 (1989).

[11] H. H. Farrell *et al.*, J. Vac. Sci. Technol. B **8**, 884 (1990).

[12] C. H. Park and D. J. Chadi, Phys. Rev. B **49**, 16 467 (1994).

[13] G. P. Lopinsky *et al.*, Surf. Sci. **355**, L355 (1996).

[14] Under the above assumptions, and using the atomistic models employed in Ref. 9 for the $c(2\times2)$ and 2×1 reconstructions, given the Zn 3*d* emission intensity from a single (100) plane of Zn atoms I^0_{Zn}, the Se 3*d* emission intensity from a single (100) plane of Se atoms I^0_{Se}, using 1 ML=1.417 Å as the interplanar spacing in bulk ZnSe, one finds $R_{c(2\times2)}=I^0_{Zn}/I^0_{Se}$, $R_{2\times1}=(I^0_{Ze}/I^0_{Se})k$, and $R_{1\times1}=(I^0_{Ze}/I^0_{Se})\cdot\{k[1-x(1-k)]/[1+kx(1-k)]\}$, where $k=e^{-1.417/\lambda}$ and x is the excess Se coverage (in ML) for the 1×1 surface relative to the 2×1 surface. Using the experimental R values for the three surfaces at a photon energy of 120 eV, we find $x=0.41\pm0.18$ ML and $\lambda=5.9\pm1.0$ Å.

[15] W. Chen *et al.*, J. Vac. Sci. Technol. B **12**, 2639 (1994).

[16] We used the pseudopotentials (nonlocal form) by R. Stumpf, X. Gonze, and M. Scheffler, Fritz-Haber-Institut Research Report No. 1, 1991 (unpublished). A nonlinear core correction was used for Zn.

[17] We used the theoretical lattice parameters $a_0^{ZnSe}=5.46$ Å and $a_\perp^{Al}=4.15$ Å, and the metal-semiconductor spacing at the junction was taken as the average of the interlayer spacings in ZnSe and Al.

[18] Atomic interdiffusion, Al-Zn exchange reactions, and Zn segregation within the Al overlayer, for example, have all been reported for Al/ZnSe junctions, (Refs. 1, 8, 10, and 15) and are largely neglected here.

[19] O. Zakharov *et al.*, Phys. Rev. B **50**, 10 780 (1994).